

## Conductive Molecular Silicon

Rebekka S. Klausen,<sup>†</sup> Jonathan R. Widawsky,<sup>‡</sup> Michael L. Steigerwald,<sup>†</sup> Latha Venkataraman,<sup>\*,‡</sup> and Colin Nuckolls<sup>\*,†</sup>

<sup>†</sup>Department of Chemistry, Columbia University, New York, New York 10027, United States

<sup>‡</sup>Department of Applied Physics and Applied Mathematics, Columbia University, New York, New York 10027, United States

### Supporting Information

**ABSTRACT:** Bulk silicon, the bedrock of information technology, consists of the deceptively simple electronic structure of just Si–Si  $\sigma$  bonds. Diamond has the same lattice structure as silicon, yet the two materials have dramatically different electronic properties. Here we report the specific synthesis and electrical characterization of a class of molecules, oligosilanes, that contain strongly interacting Si–Si  $\sigma$  bonds, the essential components of the bulk semiconductor. We used the scanning tunneling microscope-based break-junction technique to compare the single-molecule conductance of these oligosilanes to those of alkanes. We found that the molecular conductance decreases exponentially with increasing chain length with a decay constant  $\beta = 0.27 \pm 0.01 \text{ \AA}^{-1}$ , comparable to that of a conjugated chain of C=C  $\pi$  bonds. This result demonstrates the profound implications of  $\sigma$  conjugation for the conductivity of silicon.

Bulk silicon exclusively contains Si–Si  $\sigma$  bonds; indeed, the material can be imagined as a series of one-dimensional chains of Si atoms cross-linked in three dimensions. It was first shown in the middle of the 20th century that short chains of Si atoms (oligosilanes) have markedly different electronic properties than their structural analogues, the alkanes.<sup>1</sup> While alkanes do not absorb light above 190 nm, Gilman et al.<sup>2</sup> observed that permethyloligosilanes (e.g., hexamethyldisilane and higher oligomers) display strong absorbance at 200–300 nm. In a trend similar to those for linearly conjugated systems such as oligoenes,<sup>3</sup> the position of maximum absorbance ( $\lambda_{\text{max}}$ ) and the absorption coefficient ( $\epsilon$ ) increase with the length of the Si chain.<sup>2,4</sup> This observation led to speculation that saturated oligosilanes may undergo electron-transfer chemistry similar to that of conjugated carbon-based materials. Indeed, the pioneering work of West established that the stable delocalized dodecamethylcyclopentasilane radical anion can be observed by EPR spectroscopy<sup>5</sup> and that linear and cyclic oligosilanes form charge-transfer complexes with  $\pi$  acceptors such as tetracyanoethylene (TCNE).<sup>6</sup>

These promising initial experiments inspired considerable interest in the development of polymeric silanes as electronic materials; however, the challenges in silane synthesis ultimately hindered the widespread study of oligo- and polysilanes after the 1980s.<sup>7–9</sup> High-molecular-weight polymers are obtained via sodium-mediated Wurtz-type coupling of dichlorosilane monomers. The harsh conditions limit the functional group tolerance

to relatively inert alkyl and aryl substituents,<sup>10</sup> and the resultant polymers also suffer from low yields and/or wide molecular weight distributions.<sup>11</sup> Herein we report the synthesis of oligomeric silanes of specific length functionalized with anchor groups, enabling single-molecule conductance measurements. We carried out these conductance measurements on a set of SiMe<sub>2</sub> oligomers terminated with 4-(methylthio)phenyl groups (Figure 1), which bind to undercoordinated Au to form single-

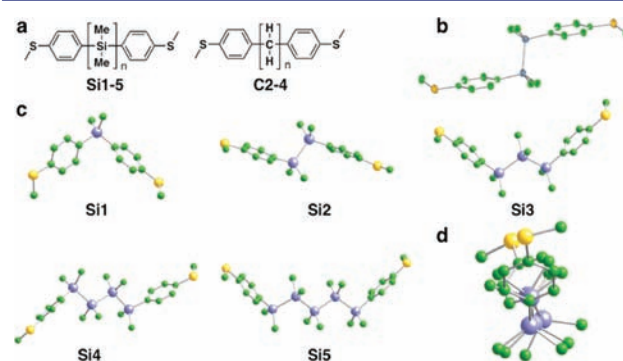


**Figure 1.** (a) Molecular structures of methyl sulfide-capped oligosilanes Si1–5 and alkanes C2–4. (b) ORTEP of a single molecule of silane Si2. Ellipsoids are shown at the 50% probability level. (c) B3LYP/6-31G\*\* calculated lowest-energy structures of oligosilanes Si1–5. (d) Perspective drawing of the lowest-energy conformation of pentasilane Si5, demonstrating the flexible silicon backbone. In (b–d), H atoms have been omitted for clarity; S is shown in yellow, Si in blue, and C in green.

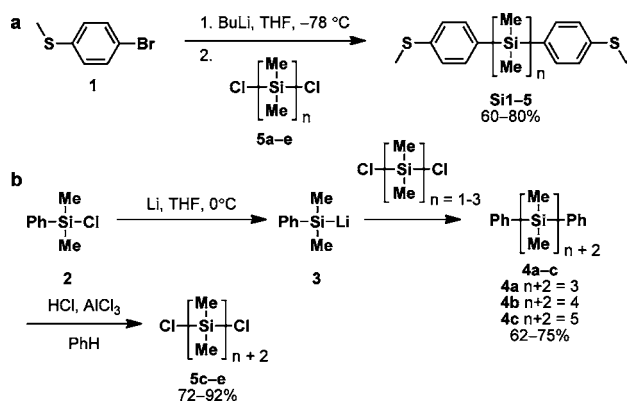
molecule junctions with linear silane backbones that are stable under ambient conditions.<sup>12,13</sup>

We synthesized the oligomeric materials via silylation of an aryllithium reagent with symmetric  $\alpha,\omega$ -dichlorooligosilanes Sa–e (Scheme 1A).  $\alpha,\omega$ -Dichlorooligosilanes are a known class of molecules and are typically synthesized by chlorination of dodecamethylcyclohexasilane.<sup>14</sup> This method yields a complex mixture of chlorosilanes that we found to be cumbersome. Instead, we employed an iterative synthesis of the  $\alpha,\omega$ -dichlorooligosilanes 5c–e in which dimethylphenylsilyllithium (3)<sup>15</sup> was coupled to commercially available dichlorodimethylsilane (5a) or dichlorotetramethyldisilane (5b) to yield  $\alpha,\omega$ -diphenyloligosilanes 4a and 4b (Scheme 1B). Protodesilylation with HCl/AlCl<sub>3</sub> yielded  $\alpha,\omega$ -dichlorooligosilanes 5c and 5d,

Received: December 29, 2011

Published: February 21, 2012

**Scheme 1. Synthetic Scheme for  $\alpha,\omega$ -Bis(4-methylthio)phenyloligosilanes Si1–5: (a) Arylsilylation Reaction; (b) Synthesis of  $\alpha,\omega$ -Dichlorooligosilanes 5c–e**



which could then be coupled with the aryl lithiates or with silyllithium **3** to yield pentasilane **4c**.<sup>16</sup> The arylsilylation reaction efficiently yielded the bis(4-(methylthio)phenyl)silanes in 60–80% yield. These compounds are air-stable solids that are soluble in common organic solvents, including hydrocarbon, aromatic, and chlorinated solvents. The crystal structure of disilane **Si2** (Figure 1B) confirmed that the Si chain adopts a fully staggered *trans* conformation, which is expected to have the optimal orbital overlap for electronic communication.<sup>17,18</sup> It is also important to note that there was no detectable decomposition or oxidation during the break-junction measurements.

The conductance of these oligosilanes **Si1–5** was measured using a scanning tunneling microscope-based break-junction (STM-BJ) technique.<sup>12,19</sup> This was carried out using a gold tip and substrate to form and break gold point contacts repeatedly in solutions of the target compounds (1 mM) in 1,2,4-trichlorobenzene. The conductance (current/voltage) was measured across the Au tip/substrate pair as a function of the tip/substrate separation. The conductance traces showed plateaus at integer multiples of  $G_0$ , the quantum of conductance, that correspond to multiples of Au atoms. At

conductance values below  $G_0$ , molecule-dependent plateaus were observed (Figure 2A inset). Thousands of traces were measured and used to generate two-dimensional (2D) conductance–displacement histograms without data selection.<sup>20,21</sup> Figure 2A shows such a 2D histogram for **Si1** that was generated with 27 000 traces [2D histograms for the other compounds are shown in the Supporting Information (SI)]. We see an intense peak around  $10^{-4}G_0$  that extends for a distance of ca. 0.5 nm, indicating that single-molecule junctions are formed reproducibly with this molecule and can be elongated over that distance.

One-dimensional conductance histograms generated using logarithm bins for the five silanes studied are shown in Figure 2B. A broad peak in each histogram at a molecule-dependent conductance value was observed (black arrows). The peak broadness is attributed to conductance variation from junction to junction, primarily due to variations in the Au–S–C torsional angle.<sup>22,23</sup> The peak positions are plotted in Figure 2C on a semilogarithmic scale against  $L$ , the effective length of the silane (the distance between the carbons para to the methylthio substituent). We see that the conductance decreased exponentially with increasing  $L$  for the first four silanes in this series (i.e.,  $G \sim e^{-\beta L}$  with  $\beta = 0.27 \pm 0.01 \text{ \AA}^{-1}$ ).<sup>24</sup> The decay constant measured here is different than the value measured in a study of photoinduced electron transfer in porphyrin–silane–fullerene dyads ( $\beta = 0.16 \text{ \AA}^{-1}$ ).<sup>25</sup> Excited-state relaxation and low-bias molecular conduction are fundamentally different processes. This  $\beta$  value compares favorably to  $\beta$  values observed for conjugated olefins, which range from 0.17–0.27  $\text{\AA}^{-1}$ .<sup>23,26</sup> The statistically determined conductance of the pentasilane **Si5** fell below this line, as can be seen in Figure 2C. We attribute this small decrease in conductance for **Si5** to its slightly twisted backbone structure,<sup>27</sup> as determined from density functional theory (DFT) calculations (Figure 1D), which decreases the “conjugation” of this molecule, similar to *gauche* defects in alkane backbones.<sup>28</sup> Notably, the difference in through-space length between *trans*-**Si5** and the twisted conformer shown in Figure 1D is insignificant.

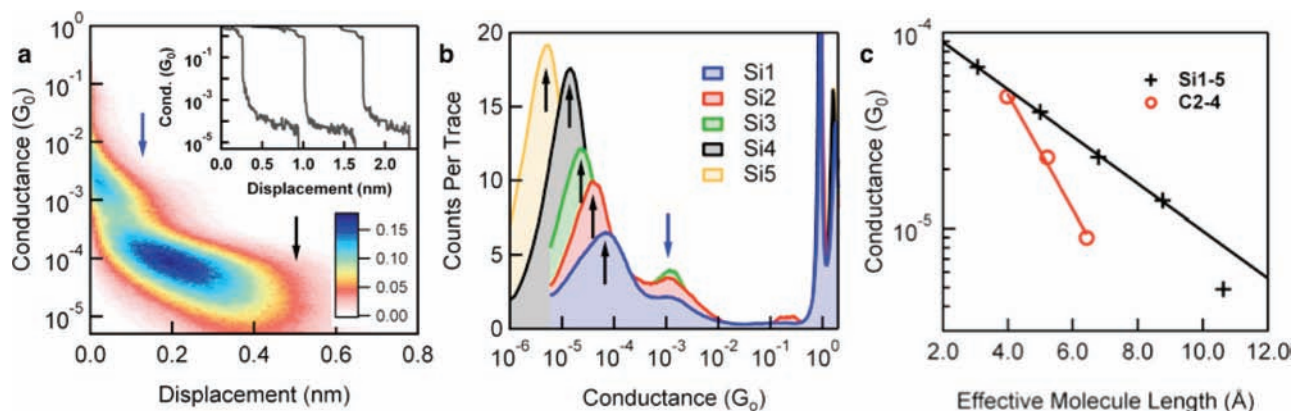


**Figure 2.** (a) 2D conductance histogram for **Si1** showing a clear conductance peak that extends over a distance of 0.5 nm relative to the break of the  $G_0$  contact. The histogram binning is 100 per decade of conductance for the y-axis and 0.0079 nm for the x-axis. The scale bar shows points per trace. The inset shows individual conductance traces. (b) Logarithm-binned conductance histograms generated using a bin size of 100/decade for compounds **Si1–5**. (c) Conductance peak values of the single-molecule junctions for the **Si $n$**  (black) and **C $n$**  (red) series as functions of the effective molecular length ( $L$ , in  $\text{\AA}$ ), defined as the distance between the carbons para to the methylthio substituent.  $L$  was determined from crystal structures Chem3D and DFT calculations. The values thus obtained varied insignificantly (<3%). The measured decay constants  $\beta$  were  $0.27 \pm 0.01 \text{ \AA}^{-1}$  for **Si $n$**  and  $0.68 \pm 0.05 \text{ \AA}^{-1}$  for **C $n$** .

Figure 2B shows that in addition to a strong molecule-dependent peak, all of these histograms had a less intense peak at ca.  $10^{-3}G_0$  (blue arrows in Figure 2A,B). The 2D histogram indicates that this peak corresponds to conductance features occurring immediately after the single-atom contact is broken at a short tip/sample displacement. Although the origin of this high-conductance feature is not fully understood, control experiments using molecules with only one terminal methyl sulfide or no anchor groups were conducted to test whether the molecule interacts with gold through the Si backbone, in analogy with an oligoene potentiometer.<sup>23</sup> Neither molecule showed clear conductance signatures (see the SI for synthesis and conductance histograms), demonstrating that in fact both sulfides are required for junction formation. Another possibility is that a cis conformation of the molecule in which the thioanisole moieties are stacked could be formed at a short electrode displacement, leading to a higher conductance with a short molecular plateau length. In support of this hypothesis, we offer the fact that conductance through the  $\pi$ - $\pi$  stack in cyclophanes has been recently reported<sup>29</sup> and that this hypothesis accounts for the observation of the same  $10^{-3}G_0$  peak in an analogous alkane series (see below).

These conductance results confirm the prediction first advanced several decades ago that while silanes are structural analogues of alkanes, their electronic properties are far more similar to those of conjugated, unsaturated hydrocarbons.<sup>1</sup> The conductance of oligosilanes Si1–5 relative to that of alkanes C2–4 inspired us to investigate electronic communication between the terminal sulfur atoms in these molecules. We performed DFT-based calculations (B3LYP/6-31G\*\*) on Si1–5 and found in each case that the highest occupied molecular orbital (HOMO) is distributed evenly across the silicon chain, the  $\pi$  systems of the arenes, and the  $p\pi$  orbitals of the two sulfur atoms.<sup>30</sup> The HOMO of Si4 is depicted in Figure 3 as a representative example. The contrast with the carbon analogue C4 is dramatic: there is essentially no electron density along the C–C backbone, and the HOMO is localized exclusively on the thioanisole fragments. In contrast, the HOMO of a butadiene terminated with 4-(methylthio)phenyl groups (6) is fully delocalized, as in the silane, indicating that

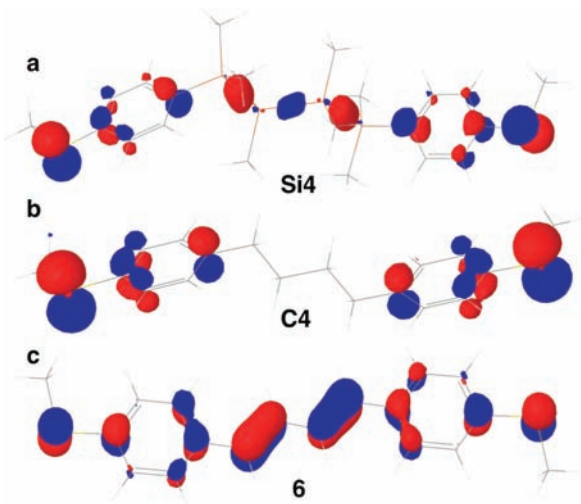


**Figure 3.** B3LYP/6-31G\*\*.-calculated HOMOs of (a) tetrasilane Si4, (b) butane C4, and (c) 1,4-bis(4-(methylthio)phenyl)buta-1,3-diene (6).

the two sulfur  $p\pi$  orbitals couple much more strongly across the Si–Si and C=C bonds than the C–C bond.

To elucidate the greater coupling observed in the Si–Si and C=C materials, we separated the molecular conductors into their constituent components: the 4-(methylthio)phenyl end groups and the conducting oligomer.<sup>31,27b</sup> Computational analysis of each part was conducted (see Table S3 in the SI). We found that the HOMOs of tetrasilane and butadiene are delocalized over the respective C and Si atoms. The HOMO level of 4-methylthioanisole lies at  $-5.49$  eV with respect to vacuum, and it is a close combination of the  $p\pi$  lone pair on S and the  $\pi$  space on the ring. We found that of the three oligomers investigated, the tetrasilane (HOMO =  $-5.96$  eV) and butadiene (HOMO =  $-5.60$  eV) lie closest in energy to that of the 4-methylthioanisole, suggesting that extensive mixing of the thioanisole and Si–Si orbitals [ $\sigma(\text{Si–Si})$ - $\pi$  conjugation] occurs; moreover, Figure 3 demonstrates that the orbital mixing is geometrically accessible.<sup>32</sup> The HOMO of hexane lies at the substantially lower energy of  $-8.29$  eV, resulting in very minimal mixing of the  $\sigma$  framework and the thioanisole orbitals [negligible  $\sigma(\text{C–C})$ - $\pi$  conjugation]. As a result, the HOMO of C4 is localized on the thioanisole. Our results indicate that uniform delocalization of the HOMO over the entire molecule improves the conductance. Consistent with this observation, a siloxane variant of Si2 was synthesized in which the Si chain is disrupted with an O atom; no conductance peak was observed (see the SI for the synthesis, conductance histogram, and HOMO calculation). We also note in passing that differential orbital coupling may account for the difference in contact resistance observed for alkanes and oligosilanes, as seen in Figure 2C.

We have presented a quantitative comparison of the conductive properties of oligosilanes and alkanes that was enabled by straightforward synthetic access to silanes functionalized with aurophilic contact groups. We have found that saturated Si nanowires display a very slow decay of conductance with length; the decay constant is comparable to that of polyacetylene fragments (oligoenes) and considerably less than those of alkane structural analogues. These results, coupled to our theoretical studies, highlight the important role of  $\sigma$ -bond conjugation in charge transport through Si–Si  $\sigma$  bonds. Currently the application of Si oligomers and polymers in electronic devices is limited,<sup>8</sup> while applications of conjugated carbon-based materials such as polyacetylene are ubiquitous.<sup>33</sup> The materials described herein have promising physical properties that are complementary to those of rigid, conjugated systems, including conformational flexibility, air and thermal stability, and high solubility in common organic solvents. We expect that the desirable physical properties and high conductance of the materials described herein will result in the development of novel molecular devices and nanoscale architectures.

## ■ ASSOCIATED CONTENT

### 📄 Supporting Information

Synthetic methods and procedures, characterization data, electrochemical and spectroscopic characterization, computational data, and crystallographic data (CIF). This material is available free of charge via the Internet at <http://pubs.acs.org>.

## ■ AUTHOR INFORMATION

### Corresponding Author

lv2117@columbia.edu; cn37@columbia.edu

## Notes

The authors declare no competing financial interest.

## ACKNOWLEDGMENTS

STM-BJ experiments were supported as part of the Center for Re-Defining Photovoltaic Efficiency Through Molecular-Scale Control, an Energy Frontier Research Center funded by the U.S. Department of Energy (DOE), Office of Science, Office of Basic Energy Sciences under Award DE-SC0001085. L.V. thanks the Packard Foundation for support. We acknowledge Yi Rong and Ged Parkin (Columbia University) for single-crystal X-ray diffraction of compound **Si2**. The National Science Foundation (CHE-0619638) is thanked for acquisition of an X-ray diffractometer. We acknowledge Roger A. Lalancette (Department of Chemistry, Rutgers University) for the **Si4** X-ray data and solution of the structure. We also acknowledge support by NSF-CRIF Grant 0443538 for part of the purchase of the X-ray diffractometer.

## REFERENCES

- (1) West, R.; Carberry, E. *Science* **1975**, *189*, 179.
- (2) Gilman, H.; Atwell, W. H.; Schwebke, G. L. *J. Organomet. Chem.* **1964**, *2*, 369.
- (3) Hausser, K. W.; Kuhn, R.; Smakula, A.; Hoffer, M. Z. *Phys. Chem., Abt. B* **1935**, *29*, 371.
- (4) Gilman, H.; Morris, P. J. *J. Organomet. Chem.* **1966**, *6*, 102.
- (5) Carberry, E.; West, R.; Glass, G. E. *J. Am. Chem. Soc.* **1969**, *91*, 5446.
- (6) Traven, V. F.; West, R. *J. Am. Chem. Soc.* **1973**, *95*, 6824.
- (7) Miller, R. D.; Michl, J. *Chem. Rev.* **1989**, *89*, 1359.
- (8) Feigl, A.; Bockholt, A.; Weis, J.; Rieger, B. *Adv. Polym. Sci.* **2011**, *235*, 1.
- (9) David, L. D.; Djurovich, P. I.; Stearley, K. L.; Srinivasan, K. S. V. *J. Am. Chem. Soc.* **1981**, *103*, 7352.
- (10) Jones, R. G.; Holder, S. J. *Polym. Int.* **2006**, *55*, 711.
- (11) Benfield, R. E.; Cragg, R. H.; Swain, A. C. *J. Chem. Soc., Chem. Commun.* **1992**, 112.
- (12) (a) Venkataraman, L.; Klare, J. E.; Nuckolls, C.; Hybertsen, M. S.; Steigerwald, M. L. *Nature* **2006**, *442*, 904. (b) Park, Y. S.; Whalley, A. C.; Kamenetska, M.; Steigerwald, M. L.; Hybertsen, M. S.; Nuckolls, C.; Venkataraman, L. *J. Am. Chem. Soc.* **2007**, *129*, 15768.
- (13) Xu, B. Q.; Tao, N. J. *Science* **2003**, *301*, 1221.
- (14) (a) Sen, P. K.; Ballard, D.; Gilman, H. *J. Organomet. Chem.* **1968**, *15*, 237. (b) Chernyavskii, A. I.; Yu, D.; Larkin, D. Y.; Chernyavskaya, N. A. *J. Organomet. Chem.* **2003**, *679*, 17. (c) Gilman, H.; Inoue, S. *J. Org. Chem.* **1964**, *29*, 3418.
- (15) (a) George, M. V.; Peterson, D. J.; Gilman, H. *J. Am. Chem. Soc.* **1960**, *82*, 403. (b) Fleming, I.; Roberts, R. S.; Smith, S. C. *J. Chem. Soc., Perkin Trans. 1* **1998**, 1209. (c) Shibano, Y.; Sasaki, M.; Tsuji, H.; Araki, Y.; Ito, O.; Tamao, K. *J. Organomet. Chem.* **2007**, *692*, 356.
- (16) Fleming, I.; Henning, R.; Parker, D. C.; Plaut, H. E.; Sanderson, P. E. J. *J. Chem. Soc., Perkin Trans. 1* **1995**, 317.
- (17) Tamao, K.; Tsuji, H.; Terada, M.; Asahara, M.; Yamaguchi, S.; Toshimitsu, A. *Angew. Chem., Int. Ed.* **2000**, *39*, 3287.
- (18) George, C. B.; Ratner, M. A.; Lambert, J. B. *J. Phys. Chem. A* **2009**, *113*, 3876.
- (19) Venkataraman, L.; Klare, J. E.; Tam, I. W.; Nuckolls, C.; Hybertsen, M. S.; Steigerwald, M. L. *Nano Lett.* **2006**, *6*, 458.
- (20) Martin, C. A.; Ding, D.; Sorensen, J. K.; Bjornholm, T.; van Ruitenbeek, J. M.; van der Zant, H. S. J. *J. Am. Chem. Soc.* **2008**, *130*, 13198.
- (21) Quek, S. Y.; Kamenetska, M.; Steigerwald, M. L.; Choi, H. J.; Louie, S. G.; Hybertsen, M. S.; Neaton, J. B.; Venkataraman, L. *Nanotechnol.* **2009**, *4*, 230.
- (22) Park, Y. S.; Widawsky, J. R.; Kamenetska, M.; Steigerwald, M. L.; Hybertsen, M. S.; Nuckolls, C.; Venkataraman, L. *J. Am. Chem. Soc.* **2009**, *131*, 10820.
- (23) Meisner, J. S.; Kamenetska, M.; Krikorian, M.; Steigerwald, M. L.; Venkataraman, L.; Nuckolls, C. *Nano Lett.* **2011**, *11*, 1575.
- (24) (a) Griffiths, D. J. *Introduction to Quantum Mechanics*, 2nd ed.; Pearson Prentice Hall: Upper Saddle River, NJ, 2005; Chapter 8. (b) Salomon, A.; Cahen, D.; Lindsay, S.; Tomfohr, J.; Engelkes, V. B.; Frisbie, C. D. *Adv. Mater.* **2003**, *15*, 1881.
- (25) Sasaki, M.; Shibano, Y.; Tsuji, H.; Araki, Y.; Tamao, K.; Ito, O. *J. Phys. Chem. A* **2007**, *111*, 2973.
- (26) Visoly-Fisher, I.; Daie, K.; Terazono, Y.; Herrero, C.; Fungo, F.; Otero, L.; Durantini, E.; Silber, J. J.; Sereno, L.; Gust, D.; Moore, T. A.; Moore, A. L.; Lindsay, S. M. *Proc. Natl. Acad. Sci. U.S.A.* **2006**, *103*, 8686.
- (27) (a) Albinsson, B.; Antic, D.; Neumann, F.; Michl, J. *J. Phys. Chem. A* **1999**, *103*, 2184. (b) Schepers, T.; Michl, J. *J. Phys. Org. Chem.* **2002**, *15*, 490.
- (28) Jones, D. R.; Troisi, A. *J. Phys. Chem. C* **2007**, *111*, 14567.
- (29) Schneebeli, S. T.; Kamenetska, M.; Cheng, Z. L.; Skouta, R.; Friesner, R. A.; Venkataraman, L.; Breslow, R. *J. Am. Chem. Soc.* **2011**, *133*, 2136.
- (30) Pitt, C. G.; Bock, H. *J. Chem. Soc., Chem. Commun.* **1972**, 28.
- (31) Bock, H.; Ensslin, W. *Angew. Chem., Int. Ed. Engl.* **1971**, *10*, 404.
- (32) Pitt, C. G.; Toren, E. C.; Carey, R. N. *J. Am. Chem. Soc.* **1972**, *94*, 3806.
- (33) Heeger, A. J. *Chem. Soc. Rev.* **2010**, *39*, 2354.